International Journal of Earth, Energy and Environmental Sciences
ISSN: 2517-942X
Vol:13, No:5, 2019

Delineating Concern Ground in Block Caving – Underground Mine Using Ground Penetrating Radar

Eric Sitorus, Septian Prahastudhi, Turgod Nainggolan, Erwin Riyanto

***Abstract*—**Mining by block or panel caving is a mining method that takes advantage of fractures within an ore body, coupled with gravity, to extract material from a predetermined column of ore. The caving column is weakened from beneath through the use of undercutting, after which the ore breaks up and is extracted from below in a continuous cycle. The nature of this method induces cyclical stresses on the pillars of excavations as stress is built up and released over time, which has a detrimental effect on both the installed ground support and the rock mass itself. Ground support capacity, especially on the production where excavation void ratio is highest, is subjected to heavy loading. Strain above threshold of the elongation of support capacity can yield resulting in damage to excavations. Geotechnical engineers must evaluate not only the remnant capacity of ground support systems but also investigate depth of rock mass yield within pillars, backs and floors. Ground Penetrating Radar (GPR) is a geophysical method that has the ability to evaluate rock mass damage using electromagnetic waves. This paper illustrates a case study from the Grasberg mining complex where non-invasive information on the depth of damage and condition of the remaining rock mass was required. GPR with 100 MHz antenna resolution was used to obtain images of the subsurface to determine rehabilitation requirements prior to recommencing production activities. The GPR surveys were used to calibrate the reflection coefficient response of varying rock mass conditions to known Rock Quality Designation (RQD) parameters observed at the mine. The calibrated GPR survey allowed site engineers to map subsurface conditions and plan rehabilitation accordingly.

***Keywords*—**Block caving, ground penetrating radar, reflectivity, RQD.

I. Introduction

GROUND Penetrating Radar (commonly called GPR) is a system that utilizes high resolution electromagnetics and is primarily used to investigate the shallow subsurface of Earth, building materials, and roads [1].

A GPR system consists of four major components (Fig. 1). These consist of a transmitter that emits electromagnetic waves into the ground, a receiver that measures the response, a control unit, and a display unit to view the resulting information. As each medium has its own electrical properties, if there is a break or change in material at depth, the electromagnetic waves will behave differently as they reflect and refract back to the receiver. The sequence of detected waves results in a continuous scan that traces the waves as a function of time and position. The GPR profile shows the subsurface condition of the medium being analyzed and, by assuming a velocity of the electromagnetic wave within the medium, the time axis can be converted to depth [2].

During the production and development stages of a block cave mine, geotechnical issues can occur, such as convergence, rock bursts, or ground failure, that compromise the stability of the excavations. The GPR instrumentation system plays a significant role in the consideration and planning of rehabilitation of damaged ground.

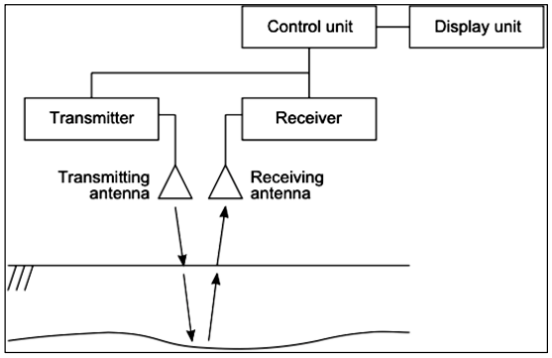

Fig. 1 Block diagram of GPR system

Signal Envelope (E) is a radargram attribute that is independent of the phase that represents amplitude of the traces, known as reflection strength. The envelope is calculated from:

$$E(t) = SQRT\{ T^2(t)+H^2(t) \}$$

where *E = Signal Envelope, T = GPR Trace, H = Hilbert's transform of T(t).* T is GPR trace and H is Hilbert's transform of T(t). The envelope is defined as the range of the received signal. It has a low frequency appearance and only positive amplitudes. By observing the envelope parameter, we could see the instantaneous energy of the signal and how the reflection coefficient is proportional with the strength of the electromagnetic signals [3]. This parameter can therefore be used to delineate areas of damaged ground within the GPR profile, details of which are then passed on to the operational team for rehabilitation work.

II. Field Description

A. Geologic Setting

The Deep Ore Zone (DOZ) ore body is located in the lower portion of the East Ertsberg Skarn System (EESS). This system consists of Tertiary-aged carbonates, altered to

Septian Prahastudhi, Turgod Nainggolan and Erwin Riyanto are with Department of Underground Geotechnical and Hydrology, Freeport Indonesia.
Eric Sitorus is with Department of Underground Geotechnical and Hydrology, Freeport Indonesia (e-mail: esitorus1@fmi.com; sitorus.ehs@gmail.com).

calcium-magnesium silicate skarn, with a vertical extent of 1200 m, length of 1000 m, and width of 200 m [4]. The skarn assemblages are locally intruded by the variably altered Ertsberg Diorite. The latter forms the footwall while forsterite skarn, magnetite-forsterite skarn, magnetite, DOZ breccia (locally known as HALO – High Altered Locally Ore), and marble are located in the hanging wall [5]. Major structures in the DOZ are primarily defined as NE-SW faults (Primary Structures) and WNW-ESE as the secondary faults.

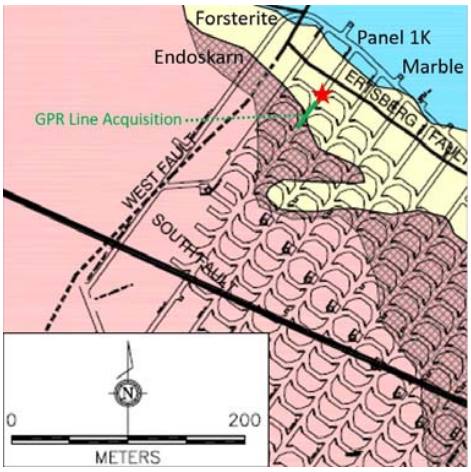

Fig. 2 DOZ Panel 1K North with GPR line acquisition (green line) and collapse area (red star icon) with lithology contact Forsterite – Endoskarn and Ertsberg fault

B. Production History of P-1K North Panel Drive, DOZ

The DOZ is a block cave mining operation that has been in production for almost 18 years. The DOZ is located approximately 900 m below surface with an average production rate of 38,000 tonnes per day, with its peak production up to 80,000 tonnes per day in 2009 and 2010. The footprint of the extraction level is 1140 m long with width ranging from 295 m to 640 m. The undercut level is located 20 m above the extraction level, which is 2590 m above sea level. While developing P-1K in the northern portion of the extraction level, a major geotechnical problem was encountered where a change in lithology intersected a significant fault zone. A collapse of the hanging wall of the extraction level occurred in the area of the fault intersection over a period of two months between February and March 2011. This was followed by a collapse of an undercut drive located directly above the panel drive in May 2011.

C. GPR Data Acquisition

Acquisition of 100 MHz frequency ZOND GPR traces have been done at the back of P-1K North's (i.e. roof), West and East Rib (side section of panel), and also West and East Shoulder (45^0 tilt from vertical) near the collapse area in 2013. The survey was conducted in drifts, with measurements performed in the ribs, shoulders, and backs for a distance of roughly 40 m (Fig. 3). To calibrate the GPR trace data, boreholes were drilled in the west rib and a camera inserted to record damaged ground and structural data.

III. GPR Reflection Model

In order to enhance the analysis result, a reflection model based on the RQD map was made. RQD is defined as the percentage of intact core pieces longer than 100 mm in the total length of core. From the RQD map, it is clear that in collapse area (Fig. 4) there are two identified ranges of RQD, those being Very Good (90%-100%) and Good (75%-90%). The damaged zone within the collapsed area is defined as Very Poor (0-25%) [6].

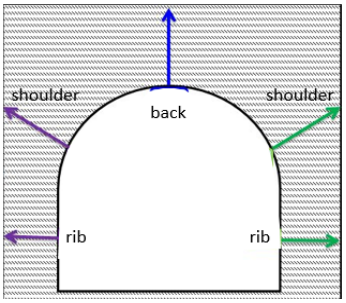

Fig. 3 Illustration of electromagnetic wave's direction on GPR acquisition in Panel 1K North

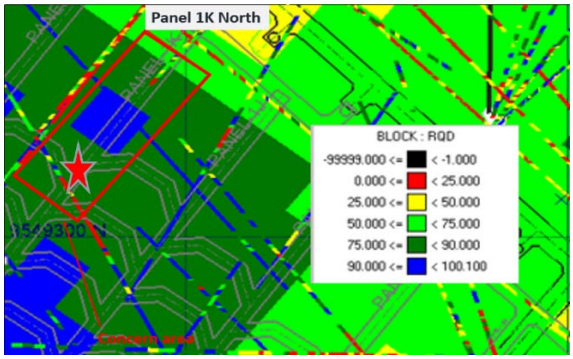

Fig. 4 RQD map in Panel 1K North. The red square zone is the concern area with red star icon is collapse area

The relation between RQD, permeability, porosity and dielectric constant can be derived using several equations.

1. From RQD to permeability (K) [7]

$$K = 0.01382 - 0.003 \ln RQD$$

2. From permeability to porosity ($\emptyset$) by using a chart's relation derived from Tiab [8]
3. From Porosity to dielectric constant (ε) [9]

$$(\varepsilon)^{0.96} = \emptyset + 6.51(1 - \emptyset)$$

The result of these calculations are that rock with Very Good RQD has a dielectric constant of 6.4, rock with a Good RQD rating is 5.9, and Poor RQD material in the damaged zone is 3.6.

The GPR reflection model processed with MATLAB (Fig. 5) shows that the waves reflection when transitioning between Very Good and Good RQD rock would show only as a small,

difficult to distinguish anomaly. However, when the waves encounter Poor RQD rock, a much larger deviation is noted, such a deviation is easily recognizable in the GPR profile stack. This finding provided the geotechnical team with confidence that this approach is suitable for determining the depth of rock damage in underground development, as well as assisting with identifying larger structures that are hidden at the rock face.

IV. Data Processing and Results

The GPR data was processed in Prism 2.5 with standard processing stages such as background removal and filter application (Fig. 6).

The processed GPR data show some low reflectivity areas which, based on the GPR reflection model, are indicators of rock masses with Poor RQD. Fractured or broken ground was found at 0.1 m, 0.3 m, and 3 m depth within the calibration boreholes. This strengthens the correlation with GPR data that shows low reflectivity at the same depth (Fig. 7).

Applying the envelope attribute, areas of low reflection, indicating damaged ground, were clearly identified (Fig. 8).

The results, coupled with the borehole calibration, confirm that the reflectivity of the waves created by the GPR system is affected when crossing anomalies in the subsurface of excavations. In this case example, the anomalies come in the form of fractures in damaged ground. The GPR allowed to the team to map the condition of the rock mass within the ribs, shoulders, and backs of the P-1K North drive. This application and several others similar to it have given the team confidence that GPR data can be used to delineate damage areas and aid in rehabilitation work for active production areas.

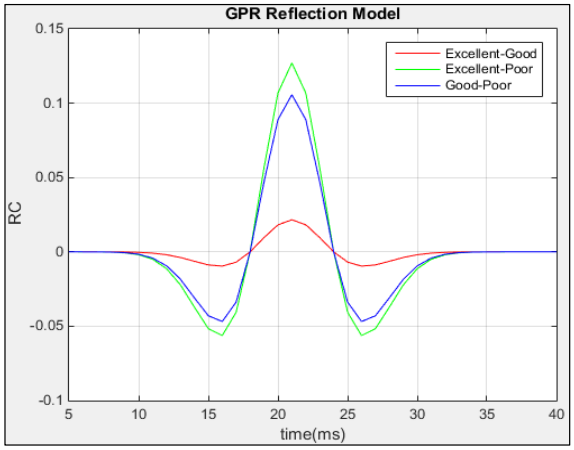

Fig. 5 GPR Reflection model when the wave propagates between Very Good RQD rock vs Good RQD rock (Red wavelet), Very Good RQD rock vs Poor RQD rock (Green wavelet), and Good RQD rock vs Poor RQD rock (Blue wavelet)

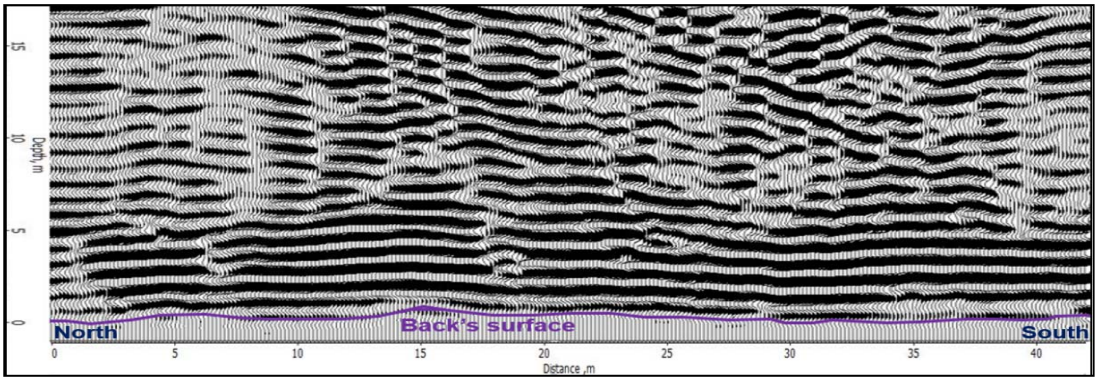

Fig. 6 Processed GPR data applied with filter and corrections in back line from North to South. Note low reflectivity zone detected

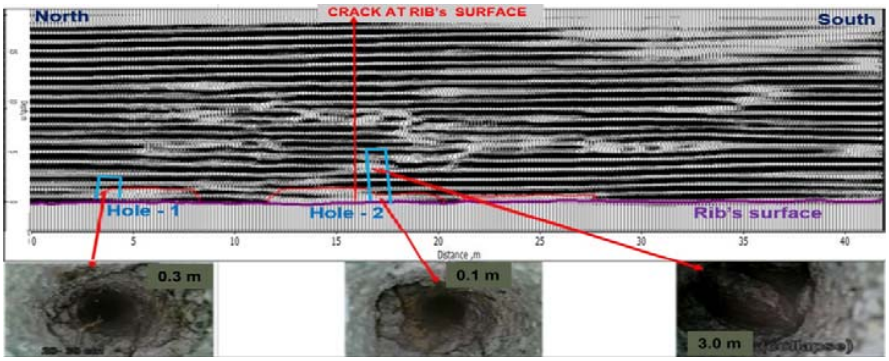

Fig. 7 Two holes were drilled into the west rib to aid in GPR calibration. The low reflectivity zones (low continuity) match well with actual ground conditions at 0.1 m, 0.3 m, and 3.0 m depth intervals where fractured and broken zones are noted

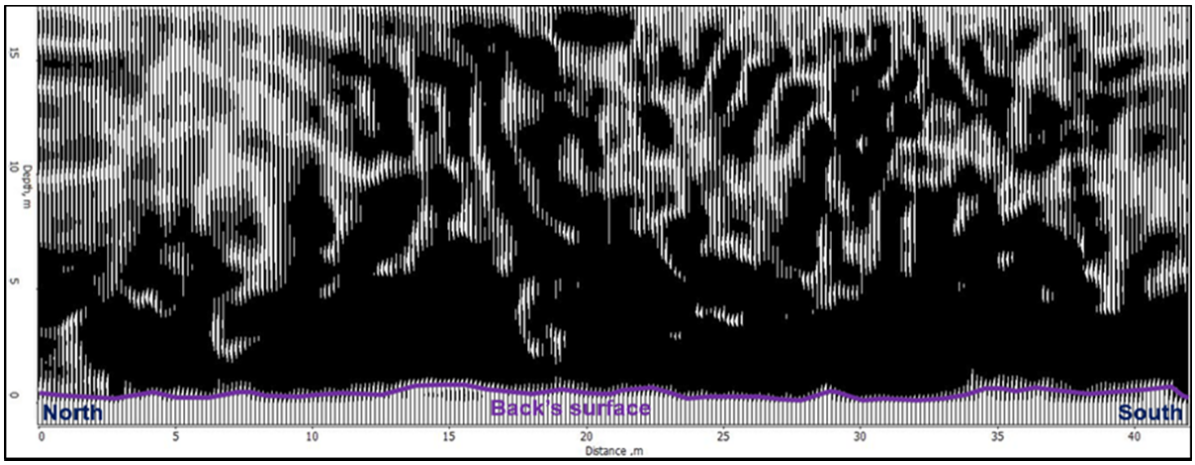

Fig. 8 GPR envelope attribute back line (up section penetration). Vertical and lateral continuity of the damage zone reflected by white to light grey colors. Collapse area in the northern end of the survey line illustrates low reflectivity

ACKNOWLEDGMENT

The authors wish to thank Underground Geotechnical DOZ and Underground Geology DOZ teams for assistance with data, and the Underground Micro-seismic and Monitoring teams for data acquisition and general support of this study.

REFERENCES

[1] Daniels, Jeffrey (2000). Ground Penetrating Radar Fundamentals. Appendix report of U. S. EPA, Region V.
[2] Takahashi, Kazunori (2010). Basics and Application of GPR as a Tool for Monitoring Irrigation Process. Problems, Perspective and Challenges of Agricultural Water Management. Willey publisher, p-155.
[3] Subrahmanyam, D (2008). Seismic Attributes – A Review. 7th International Conference and Exhibition on Petroleum Geophysics, p-398.
[4] T Casten, J Barber, L Thomas. (2000). Freeport Indonesia's Deep Ore Zone Mine. MassMin 2000. pp. 289-294.
[5] Coutts BP, Susanto H, Belluz N, Flint D, Edwards A, (1999). Geology of the Deep Ore Zone, Ertsberg East Skarn System, Irian Jaya. AusIMM PACRIM Conference 1999. pp. 539-547.
[6] Hoek, E (2013). Quantification of the Geological Strength Index Chart. Bulletin of American Rock Mechanic Association. 47. pp. 663-672.
[7] Qureshi M. U., Khan K. M., Bessaih N., Al-Mawali K. & Al-Sadrani K. 2014. An empirical relationship between in-situ permeability and RQD of discontinuous sedimentary rocks, Electronic Journal of Geotechnical Engineering, Vol.19/R, pp.4781-4790.
[8] Tiab, Djabar and Donaldson, Erle (1996). Petrophysics: Theory and Practice of Measuring Reservoir Rock and Fluid Transport Properties, Gulf Professional Publishing.
[9] Rust, A (1999). Dielectric constant as a predictor of porosity in dry volcanic rocks. Journal of Volcanic and Geothermal Research. pp. 79-96.